IEEE Access
Multidisciplinary | Rapid Review | Open Access Journal

Received January 30, 2019, accepted March 20, 2019, date of publication March 25, 2019, date of current version April 12, 2019.

Digital Object Identifier 10.1109/ACCESS.2019.2907137

A Quantum State Controller Based on the Electromagnetic Potentials

CHEN XIANG, FANMING KONG, KANG LI, (Member, IEEE), AND MENG LIU
School of Information Science and Engineering, Shandong University, Qingdao 266237, China

Corresponding author: Kang Li (kangli@sdu.edu.com)

This work was supported by the National Key R&D Program of China under Grant 2016YFC0302802.

ABSTRACT Based on the Maxwell–Schrödinger system, a novel numerical scheme for controlling the quantum states of a single electron is proposed in this paper. The key ingredient of the scheme is to employ the electromagnetic potentials instead of the conventional fields for avoiding extra steps of the simulation. The relevant perfect matched layer is given to simulate seemingly infinite regions. And with the help of precise transfer between the objective and the start state, a control pulse can be designed to accurately excite the particle into the objective state. The proposed scheme can perform an ideal quantum state switching while of a simple numerical process.

INDEX TERMS Maxwell-Schrödinger equations, quantum state control, perfect matched layer, finite-difference time-domain.

I. INTRODUCTION

Recent technology development in quantum regions has opened a way to control quantum states of electrons, atoms, molecules, and nano-scale objects [1]. These studies have attracted great attention over the past 20 years since they seem to have the ability to control photochemical reactions with high efficiency. But this pioneering technology needs to design external laser pulses to the target systems, which are not that simple to figure out through the basic quantum theories [2]. Hence, optical control of states through computational algorithm has been a growing interest in recent years [3]–[5]. These have prompted demand for new analysis technique of electrical structures in nano-scale where quantum effects have to be considered. The time and memory cost should be also taken into account for long time simulations.

We note here that many researchers have done precursory and strict works where Maxwell's equations are directly involved in the solutions. Since the Maxwell's and Schrodinger's equations are both time- and spatial-domain differential, finite-difference time-domain (FDTD) method and its variants have been proved to be the most efficient, concise and employed [6], [7]. In the attempts to easily generate the designed control pulse, many groups have done excellent works, like the genetic algorithm [5] and the light-control scheme based on optimal control theory [8], [9]. The group demonstrates that, under the certain genetic algorithm, the pulse can be collected through a liquid-crystal phase modulator. The optimal control theory adds a new dimension to design the control pulse. However, all of above seem to rely on the assumption that the electromagnetic fields near the atoms would not be disturbed by atoms excitation or the disturbance can be negligibly tiny to be ignored [10]. But the excited electron by the incident pulse is a superposition of several states and becomes a local current source which can radiate new electromagnetic waves [11], [12]. Thus, the fields near the electron should be the sum of the incident waves and the new radiated ones.

Since the Schrödinger equation gets electric scalar potential and magnetic vector potential involved instead of the electromagnetic fields, the researchers cannot avoid the steps where the potentials are extracted from the fields with conventional Maxwell FDTD methods employed [6], [7], [13]–[15]. A group introduces the length gauge [16] which can transform the quantum system into a scheme with the electromagnetic fields directly involved, trying to avoid the additional steps of potential-field extraction [17]. However, this gauge is under the dipole approximation, namely, assuming the position effects of the vector potential is neglected. This approximation makes the length-gauge inaccurate in short wavelength simulations [17], [18].

The associate editor coordinating the review of this manuscript and approving it for publication was Siddhartha Bhattacharyya.

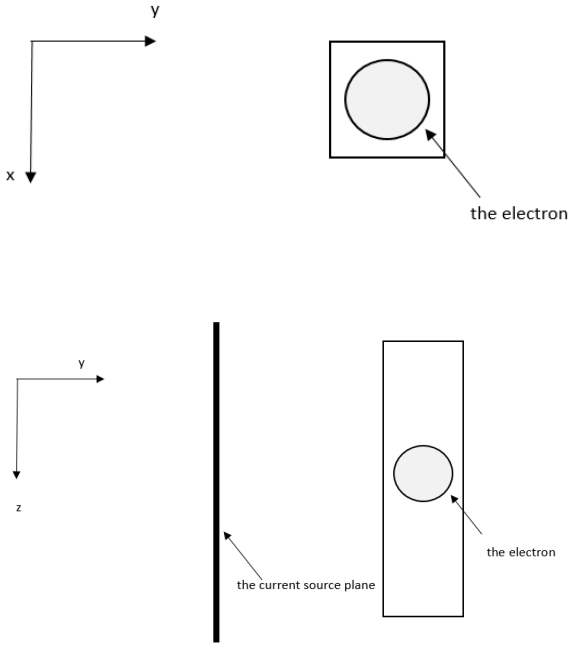

FIGURE 1. The geometry and coordinates of the quasi-one-dimensional system.

C. Ryu at el propose a novel system where the electromagnetic potentials are directly iterated, but the PML regions are complicated [19].

This hybrid simulation of the coupled electromagnetic-potentials-Schrodinger equations form a novel computational algorithm, aimed to accelerate the simulation without unnecessary assumptions. This scheme focuses on the system of a single particle, and studies the quantum states of the particle effected by electromagnetic incident pulses. The results shows the pulses can lead to the change of the states accurately.

II. NUMERICAL MODELS

In this study, we use an electron system where the particle is confined in a quasi-one-dimensional space and try to generate the pulses which can transfer the probability density into the wanted state. Hence the wavefunction of the system will be one-dimensional and convenient to obtain the variations of the wavefunction or the probability density in time- and spatial- domain. The geometry and coordinates of the system are schematically shown in Figure 1. The designed control pulse source is uniform for the XZ- plane and polarized along the z- axis.

The control pulse equation of our algorithm is developed from the valid method which is proved to be accurate and efficient to transform the ground state to the wanted state [18], [20]. And then the system is employed in the conventional length gauge scheme, the conventional Maxwell-Schrödinger scheme, and our proposed scheme.

A. THE MAXWELL-SCHRODINGER SCHEME

The wavefunction of the quasi-one-dimensional system can be described by the modified Schrödinger equation with the z- component of the magnetic vector potential $\vec{A}$ and the scalar potential Φ involved:

$$i\hbar\frac{\partial}{\partial t}\Psi(z,t) = \frac{\hbar}{2m}\{[-i\hbar\frac{\partial}{\partial z} - qA_z]^2 + q\Phi + V\}\Psi(z,t) \quad (1)$$

where $\hbar$ represents Planck's constant; q is the charge of the particle; m denotes the effective mass of the particle; Ψ represents the wavefunction of the system, and $|\Psi|^2$ is the probability density function of the particle; V denotes the confinement potential.

To obtain the above potentials, the well-known Maxwell's equations are introduced to get the electromagnetic fields at first,

$$\nabla \times \vec{E} = -\mu\frac{\partial \vec{H}}{\partial t} \quad (2)$$

$$\nabla \times \vec{H} = \varepsilon\frac{\partial \vec{E}}{\partial t} + J_q \quad (3)$$

The term J_q is the connection between the Maxwell part and the Schrödinger part,

$$J_q = \frac{q}{2}\{[\frac{-i\hbar - qA_z}{m}(\Psi)]^*\Psi) + (\Psi)^*[\frac{-i\hbar - qA_z}{m}(\Psi)]\} \quad (4)$$

The vector potential $\vec{A}$ and the scalar potential Φ satisfy the definition as,

$$\vec{E} = -\frac{\partial}{\partial t}\vec{A} - \nabla\Phi \quad (5)$$

Then with the famous Lorentz gauge employed, since it is simple in finite-difference time-domain (FDTD), all the above equations are coupled to each other:

$$\nabla \cdot \varepsilon\vec{A} = -\mu\varepsilon^2\frac{\partial}{\partial t}\Phi \quad (6)$$

Equation (1)-(6) is the key to the conventional Maxwell-Schrödinger system. The system is proved to be valid and suitable for state control. The equations are not closely coupled. In every step, the potentials should be extracted from the electromagnetic field to calculate the current term J_q and the Schrödinger equation. With the control pulse generator, the situation will be more complicated, as shown in Figure 2.

The control pulse generator is designed to maximize the objective state Ψ_1 of the electron from the initial state Ψ_0. And for numerical convergence, the initial state is modified with a small amount of the objective state as follows,

$$\Psi_{N1} = \sqrt{0.999999}\Psi_0 + \sqrt{0.000001}\Psi_1 \quad (7)$$

And then the pulse can be generated by solving the equation below,

$$E_z^i = -2\frac{E_0}{m}\mathrm{Im}\left\langle\tilde{\Psi}|\Psi_{N1}\right\rangle\left\langle\Psi_{N1}|qz\tilde{\Psi}\right\rangle \quad (8)$$

where E_0 is a cutoff function, $\tilde{\Psi}$ is the transformed wavefocuntion of the i-th time step.

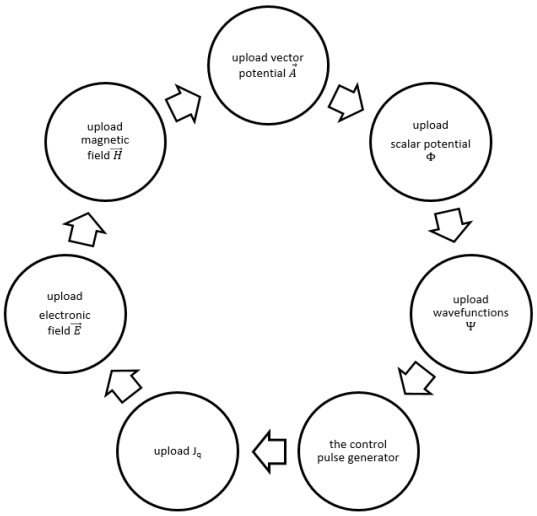

FIGURE 2. The program flow of the conventional Maxwell-Schrödinger state controller.

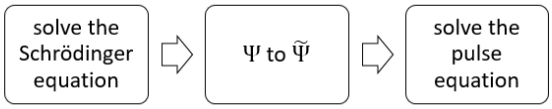

FIGURE 3. The program steps of the pulse generator.

The transformation of $\tilde{\Psi}$ is without the dipole approximation, namely,

$$\tilde{\Psi}(z,t) = \exp\{-\frac{iqA_z(z,t)}{\hbar}\}\Psi(z,t) \tag{9}$$

The steps of the pulse generator are shown in Figure 3. This scheme is certified to be accurate in [18], [20] and provides reliable results in the experimental comparison.

B. THE LENGTH GAUGE SCHEME

The aim of the length gauge scheme is to simplify the conventional Maxwell-Schrödinger system into a form without the electromagnetic potentials involved. The time-dependent Schrödinger equation can be modified by this gauge as,

$$i\hbar\frac{\partial}{\partial t}\Psi(z,t) = \frac{\hbar}{2m}[\frac{\partial^2}{\partial z^2} - qE_z(z,t)z + V]\Psi(z,t) \tag{10}$$

Once the electric fields are updated in the Maxwell part using (2) and (3), the wavefunction can be solved directly.

Since the radiation gauge is introduced in this scheme, the feedback term J_q is neglected based on the assumption that the electron motions may have much less influence than the control pulse. Then the vector potential $\vec{A}$ is independent of spatial- domain and the scalar potential Φ is confined to zero by the dipole approximation as,

$$\frac{\partial A_z}{\partial t} = -E_z \tag{11}$$

$$\Phi = 0 \tag{12}$$

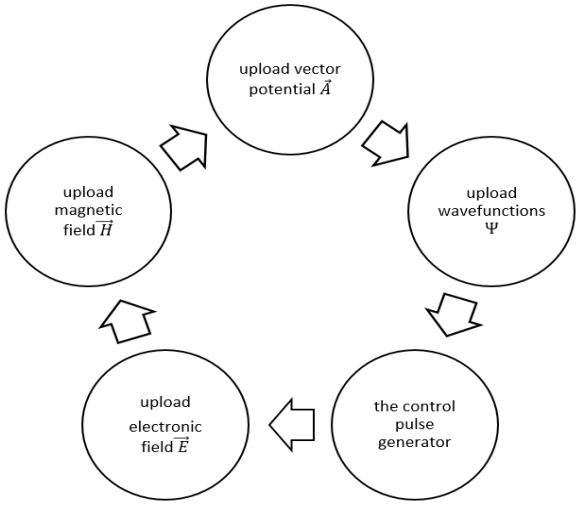

FIGURE 4. The program flow of the length gauge state controller.

Therefore, the transformation of wavefunction is simpler as,

$$\tilde{\Psi}(z,t) = \exp\{-\frac{iqA_z(t)}{\hbar}\}\Psi(z,t) \tag{13}$$

Using (2), (3) and (10-13), the length gauge scheme can work more quickly and reduce computer memory cost as illustrated in Figure 4. But this scheme seems to be unable to accurately excite the electron to the objective state. Because the excited electron motions by the pulse make the electron become a new local current source. And the new current can radiate new electromagnetic waves and affects the Maxwell part. Thus, the fields near the electron should be the cooperation between the incident pulses and the new excited one.

C. THE PROPOSED SCHEME

Our proposed scheme is aimed at simplifying the conventional Maxwell-Schrödinger system as well as constructing a precise and tightly coupled algorithm for state control. The length gauge is an attempt to get rid of the electromagnetic potentials. On the contrary, the proposed algorithm sweeps away all the terms of the electromagnetic fields and directly employs the potentials in the numerical iterations. And as the conventional perfect matched layer (PML) method is prerequisite for the conventional Maxwell system, a new hybrid PML method is developed for this scheme.

The magnetic vector potential $\vec{A}$ and the scalar potential Φ are defined as

$$H = \mu^{-1}\nabla\times\vec{A} \tag{14}$$

$$\vec{E} = -\frac{\partial}{\partial t}\vec{A} - \nabla\Phi \tag{15}$$

Equation (14) and (15) are substituted into (3),

$$\frac{\partial^2}{\partial t^2}\varepsilon\vec{A} + \frac{\partial}{\partial t}\varepsilon\nabla\Phi + \nabla\times\mu^{-1}\nabla\times\vec{A} = 0 \tag{16}$$

In order to simplify the time-domain term, the Lorentz gauge (6) is substituted into (16). So the Maxwell part of our

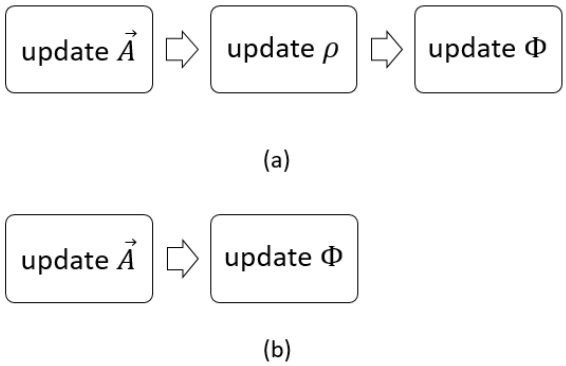

FIGURE 5. (a) The program flow of the previous potential equations, (b) the steps of the proposed Maxwell part.

system can be described by the new vector potential equation and the Lorentz gauge,

$$\frac{\partial^2}{\partial t^2}\varepsilon\vec{A} = \varepsilon\nabla\varepsilon^{-2}\mu^{-1}\nabla\cdot\varepsilon\vec{A} - \nabla\times\mu^{-1}\nabla\times\vec{A} + J_q \quad (17)$$

$$\mu\varepsilon^2\frac{\partial}{\partial t}\Phi = -\nabla\cdot\varepsilon\vec{A} \quad (18)$$

Compared with our previous work [21], these two new equations can update the potentials without the current continuity equation involved and have a succinct form for the scalar potential iterations. These advantages making the proposed method more quickly and energy-saved than our previous work. Figure 5 is the comparison between the two methods.

As the electron should be set in the region without any reflection from the boundary. So the absorbing boundary should be developed for the new coupled equations to approximate this situation and save memory cost. The PML equations for the z-component electric field can be written as,

$$\varepsilon\frac{\partial}{\partial t}E_{z_x} + \rho_{pex}E_{zx} = \frac{\partial(H_{yz}+H_{yx})}{\partial x} \quad (19)$$

$$\varepsilon\frac{\partial}{\partial t}E_{z_y} + \rho_{pey}E_{zy} = \frac{\partial(H_{xy}+H_{xz})}{\partial y} \quad (20)$$

where the electric field E_z is separated into E_{zx} and E_{zy}, the magnetic field H_x and H_y is separated into H_{xz} and H_{xy}, H_{yz} and H_{yx} respectively.

From the (14), it is easily indicated that H_{xz} and H_{yz} can be derived from the z-component of $\vec{A}$ as follows,

$$H_{yz} = -\mu^{-1}\frac{\partial}{\partial x}A_z \quad (21)$$

$$H_{xz} = \mu^{-1}\frac{\partial}{\partial y}A_z \quad (22)$$

And the other two separated magnetic fields are related with only one dimensional component of $\vec{A}$ as

$$H_{xy} = -\mu^{-1}\frac{\partial}{\partial z}A_y \quad (23)$$

$$H_{yx} = \mu^{-1}\frac{\partial}{\partial z}A_x \quad (24)$$

Equation (21-24) are substituted into (19) and (20) using the relation $E_z = E_{zx} + E_{zy}$,

$$\varepsilon\frac{\partial^2}{\partial t^2}A_z + 2\rho_{pex}\frac{\partial}{\partial t}A_z + \varepsilon[-\nabla\varepsilon^{-2}\mu^{-1}\nabla\cdot\varepsilon\vec{A}]_z + 2\rho_{pex}[\nabla\Phi]_z = -\frac{\partial^2}{\partial x\partial z}A_x + \frac{\partial^2}{\partial z\partial y}A_y \quad (25)$$

This equation can update the z-component of the vector potential in the PML region. The PML equations for the other two components of the vector potential are symmetrical with (25).

The scalar in the PML regions can be solved by introducing the coordinate stretching,

$$\nabla_s = \frac{jw\varepsilon_0}{jw\varepsilon_0+\rho_{pml}}\frac{\partial}{\partial t}\vec{x} + \frac{jw\varepsilon_0}{jw\varepsilon_0+\rho_{pml}}\frac{\partial}{\partial t}\vec{y} + \frac{jw\varepsilon_0}{jw\varepsilon_0+\rho_{pml}}\frac{\partial}{\partial t}\vec{x} \quad (26)$$

With (26) substituted into (18), the new equation in the frequency domain is written as,

$$j\omega\varepsilon_0\mu\varepsilon^2\Phi + \rho_{pml}\mu\varepsilon^2\Phi = -\varepsilon_0\nabla\cdot\varepsilon\vec{A} \quad (27)$$

Then (26) is converted into time domain, and the scalar potential in the PML regions can be obtained as follows,

$$\mu\varepsilon^2\frac{\partial}{\partial t}\Phi + \frac{\rho_{pml}}{\varepsilon_0}\Phi = -\nabla\cdot\varepsilon\vec{A} \quad (28)$$

For the Schrödinger part, the standard and time-dependent Schrödinger equation is employed in the proposed scheme,

$$i\hbar\frac{\partial}{\partial t}\Psi(z,t) = \frac{\hbar}{2m}\{[-i\hbar\frac{\partial}{\partial z} - qA_z]^2 + q\Phi + V\}\Psi(z,t) \quad (29)$$

As to sweep out the electric fields, the control pulse should be chosen as an infinite current plane instead of the incident waves. The generator equation is modified as,

$$J_z^i = -2\frac{J_0}{m}\mathrm{Im}\left\langle\tilde{\Psi}|\Psi_{N1}\right\rangle\left\langle\Psi_{N1}|qz\tilde{\Psi}\right\rangle \quad (30)$$

The cutoff function J_0 can be derived as follows,

$$J_0 = -\frac{2\eta}{\Delta x Z_0}\exp\{-\frac{t-\tau}{\gamma}u(t-\tau)\} \quad (31)$$

where Z_0 is the impedance of air, $u(t-\tau)$ denotes the unit step function; η, γ and τ are the constants chosen to be 0.5 GV/m, 30 fs and 3 fs.

Using (17), (18), (29-31), the proposed scheme can handle the simulation where a designed laser is propagating towards a quasi-one-dimensional system. When the pulse arrives, the electron is excited by the Schrödinger equation (26) under the influence of the electromagnetic potentials. Then, the motions of the electron create a new current source. This source works as a feedback to the potential system (17)-(18). Figure 6 shows the program flow of the proposed scheme. This scheme avoid the extra calculation between the potential and the fields without any approximation involved.

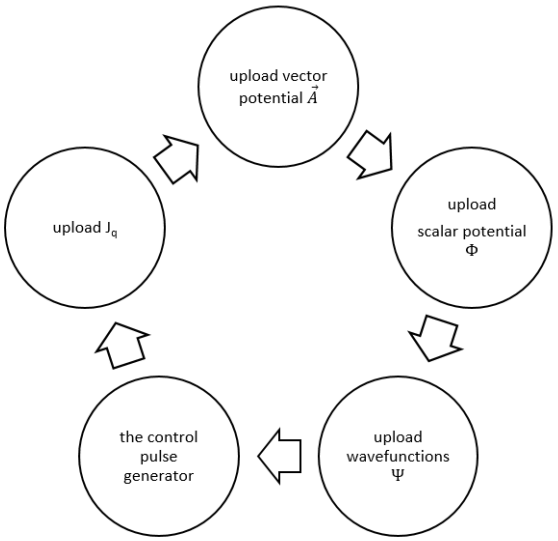

FIGURE 6. The program flow of the proposed method.

III. DISCRETIZATION OF THE PROPORSED SCHEME

In order to obtain the discretized equations of our scheme, the FDTD method is employed. In the time domain, the second-order differences are selected. But for the spatial domain, the four-order differences are chosen for higher accuracy,

$$\frac{\partial K}{\partial x} = \frac{1}{12\Delta x}[-K(i-2)+8K(i-1) -8K(i+1)+K(i+2)]+\mathrm{O}((\Delta \mathrm{x})^4) \quad (32)$$

A. THE MAXWELL POTENTIALS

Using the second-order differences in the time domain, the discretized equations for the coupled potentials (17) and (18) can be obtained as,

$$A_v^{n+1} = 2A_v^n - A_v^{n-1} + \frac{\Delta t^2}{\varepsilon}(-\varepsilon\nabla\mu^{-1}\varepsilon^{-2}\nabla\cdot\varepsilon\vec{A} + \nabla\times\mu^{-1}\nabla\times\vec{A} + (J_q^n)_v) \quad v = x, y, z \quad (33)$$

$$\Phi^{n+1} = \Phi^n - \Delta t\frac{\nabla\cdot\varepsilon\vec{A}}{\mu\varepsilon^2} \quad (34)$$

$\vec{A}$ is divided in to A_x, A_y, and A_z, and $\vec{J}_q$ is divided into $\vec{J}_{qx}$, $\vec{J}_{qy}$, and $\vec{J}_{qz}$. Unlike the conventional scheme, the scalar potentials do not need to be divided.

For (34), the term $\nabla\cdot\varepsilon\vec{A}$ can be solved directly,

$$f_1 = \nabla\cdot\varepsilon\vec{A} = \frac{\partial}{\partial x}\varepsilon A_x + \frac{\partial}{\partial y}\varepsilon A_y + \frac{\partial}{\partial y}\varepsilon A_y \quad (35)$$

In the vector updated equation (33), the remained terms should be solved. The form of term $\nabla\times\mu^{-1}\nabla\times A^n$ can be found in our previous work [21]. The term $\nabla\mu^{-1}\varepsilon^{-2}\nabla\cdot\varepsilon\vec{A}$ can be written as,

$$\nabla\mu^{-1}\varepsilon^{-2}\nabla\cdot\varepsilon\vec{A} = \nabla\mu^{-1}\varepsilon^{-2}f_1 = \vec{x}\frac{\partial}{\partial x}\mu^{-1}\varepsilon^{-2}f_1 + \vec{y}\frac{\partial}{\partial y}\mu^{-1}\varepsilon^{-2}f_1 + \vec{z}\frac{\partial}{\partial z}\mu^{-1}\varepsilon^{-2}f_1 \quad (36)$$

B. THE SCHRODINGER EQUATION

If the software is available for complex numbers, the Schrödinger equation can be discretized as follows,

$$\Psi^{n+1}(k) = \Psi^n(k) + \Delta t\frac{\hbar}{2m}\frac{\partial^2}{\partial z^2}\Psi^n(k) + \Delta t\frac{q}{m}A_z^n\cdot\frac{\partial}{\partial z}\Psi^n + \Delta t\frac{q}{2m}(\frac{\partial}{\partial z}A_z^n)\Psi^n - i\frac{\Delta t q^2}{2\hbar m}(A_z^n)^2\Psi^n(k) - i\Delta t\frac{q\Phi+V}{\hbar}\Psi^n(k) \quad (37)$$

If only real number calculations are supported, the wavefunction should be divided into its real part and imaginary part as,

$$\Psi = \Psi_R + i\Psi_I \quad (38)$$

(38) is substituted into (37), the discretized equations can be written as,

$$\Psi_R^{n+1}(k) = \Psi_R^n(k) - \Delta t\frac{\hbar}{2m}\frac{\partial^2}{\partial z^2}\Psi_I^n(k) - \Delta t\frac{q}{m}A_z^n\cdot\frac{\partial}{\partial z}\Psi_R^n - \Delta t\frac{q}{2m}(\frac{\partial}{\partial z}A_z^n)\Psi_R^n + \frac{\Delta t q^2}{2\hbar m}(A_z^n)^2\Psi_I^n(k) - \Delta t\frac{q\Phi+V}{\hbar}\Psi_I^n(k) \quad (39)$$

$$\Psi_I^{n+1}(k) = \Psi_I^n(k) + \Delta t\frac{\hbar}{2m}\frac{\partial^2}{\partial z^2}\Psi_R^n(k) - \Delta t\frac{q}{m}A_z^n\cdot\frac{\partial}{\partial z}\Psi_I^n - \Delta t\frac{q}{2m}(\frac{\partial}{\partial z}A_z^n)\Psi_I^n - \frac{\Delta t q^2}{2\hbar m}(A_z^n)^2\Psi_R^n(k) + \Delta t\frac{q\Phi-V}{\hbar}\Psi_R^n(k) \quad (40)$$

C. THE PULSE GENERATOR

The discretized formula for the current generator (30) can be written as,

$$J_{in}^n = -\frac{qJ_0\Delta z^2}{m}\{[\sum_{k=z_0}^{z_{\max}}\tilde{\Psi}_R^n(k)\Psi_{N1}(k)]\times[\sum_{k=z_0}^{z_{\max}}Z(k)\tilde{\Psi}_I^n(k)\Psi_{N1}(k)] - [\sum_{k=z_0}^{z_{\max}}\tilde{\Psi}_I^n(k)\Psi_{N1}(k)]\times[\sum_{k=z_0}^{z_{\max}}Z(k)\tilde{\Psi}_R^n(k)\Psi_{N1}(k)]\} \quad (41)$$

where Z(k) denotes the discretized z- axis.

IV. EXPERIMENTS

A. THE PML TEST

The proposed PML formulas should be tested whether the PML boundary can absorb all the energy in the simulation. A single dipole set in the infinite space is to verify that the PML regions can absorb the potentials without any reflection. The simulation domain is confined to be 84 × 84 × 278 with PML region of 20 cell thickness. The dipole is $\vec{J}_z = \vec{z}\sin(2\pi ft)$ where the frequency is 0.2GHz. The cell size of all axes is 0.3m. The analytical results and the proposed PML are compared with each other.

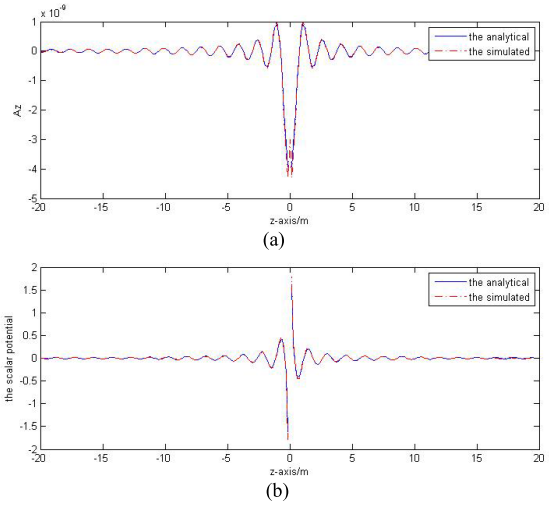

FIGURE 7. (a)The plots of the analytical vector potential of z- axis versus the simulated, (b) the plots of the analytical vector potential of z- axis versus the simulated.

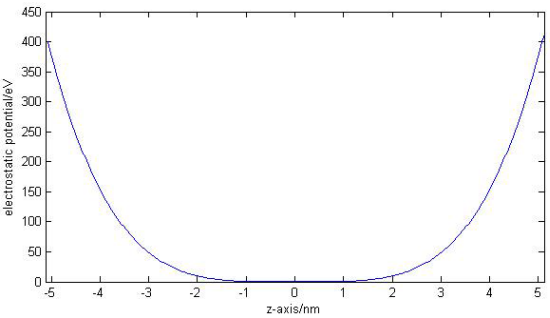

FIGURE 8. The plots of the confining potential V.

The analytical values of the single dipole are given as

$$A = \vec{z}\frac{\mu Il}{4\pi r}e^{ikr}e^{i\frac{\pi}{2}} \tag{42}$$

$$\Phi = \cos\theta\frac{Il}{4\pi r}e^{ikr}e^{i\frac{\pi}{2}} \tag{43}$$

The vector potential plots are shown in Figure 7. The differences between the theoretical value and the proposed method are mainly in the dipole position and the PML regions. The theoretical vector potential value of the position where the dipole is set should be infinite according to (42). But in numerical calculations, the potential value is the function of its previous and nearby values. So the potential value cannot arrive the infinite number. The distinct lines in the PML regions show that our proposed PML boundary can eliminate the potentials into the PML, and the values in the normal regions show little differences except for the error of the dipole position after enough number time steps.

The results verify that the proposed PML well agrees with the analytical values.

B. THE STATE CONTROL

The quasi-one-dimensional system in Figure 1 is discussed in this section. Figure 8 displays the confining potential V of the system. And the ground state Ψ_0 and the objective state Ψ_1 are illustrated in Figure 9.

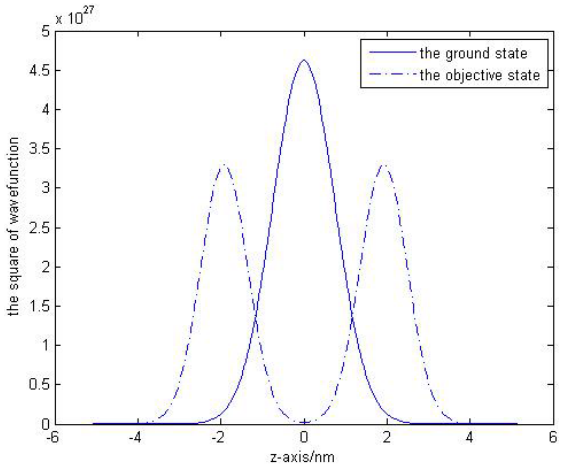

FIGURE 9. The plots of the ground state and the objective state.

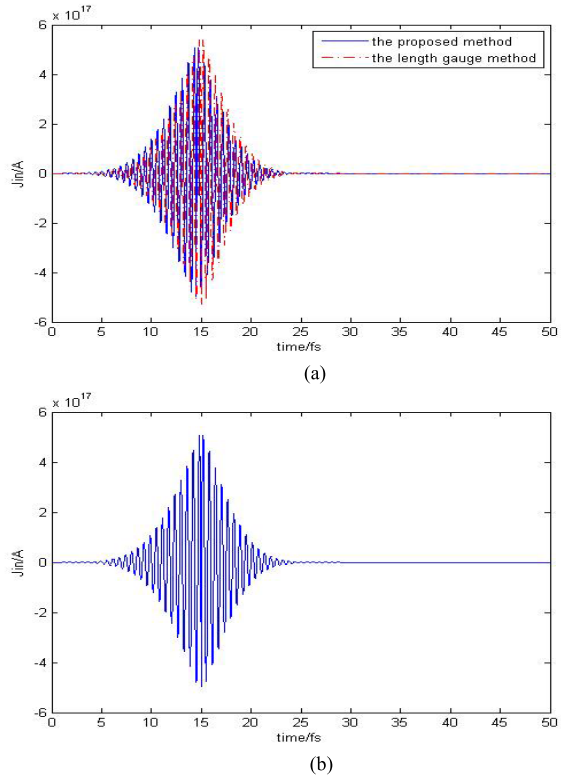

FIGURE 10. (a)The plots of the pulses by the proposed scheme and the length gauge scheme (b) the plots of the pulses of the T. Takeuchi et al scheme.

The simulation domain is $50 \times 50 \times 268$ with the PML regions of 20 cell thickness. The cell size of the z-axis is set as $\Delta z = 0.02nm$ and the cell sizes of X- and Y- axes are $\Delta x = \Delta y = 0.5nm$.

The pulses generated by the proposed scheme and the length gauge scheme are displayed in Figure 10(a). The pulses by the scheme of Takeuchi et al are shown in Figure 10(b). Notice that the pulses of our scheme and the

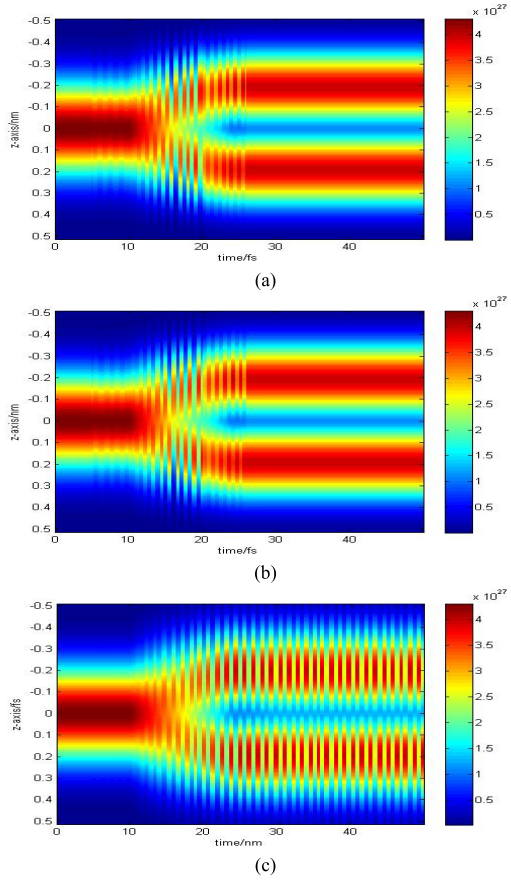

FIGURE 11. The spatiotemporal plots of the probability density $|\Psi|^2$ of (a) the proposed scheme, (b) the scheme of T. Takeuchi et al and (c) the length gauge scheme.

scheme by T. Takeuchi et al show little difference because both schemes are without dipole approximation involved. The control abilities of the two schemes are expected to be the same. The results between the proposed and the length gauge scheme show appreciable deviations, leading to different control performance.

The variation of the probability density $|\Psi|^2$ of the electron by the different schemes is displayed in Figure 11. As shown in Figure 11(a) and (b), the density starts fluctuating about the time 5 fs in the proposed and the T. Takeuchi et al scheme. Then at the periods of time 10 $\sim$ 27 fs, the distribution of the density is efficiently illuminated by the pulses and finally changed into a double peak form. There are some tiny differences between the two methods in these periods, but both two are able to reach the same and stable results. For the results of the length gauge in (c), the density never becomes identical to the objective state even after the pulses has been cut off. This indicates that if the quantum feedback is ignored, the pulses are of less control ability.

A quantitative factor Ω of the control performance in the three schemes is estimated by projecting the real-time transformed wavefunction and the objective state Ψ_1,

$$\Omega = \left\langle \tilde{\Psi} | \Psi_1 \right\rangle \left\langle \Psi_1 | \tilde{\Psi} \right\rangle \tag{44}$$

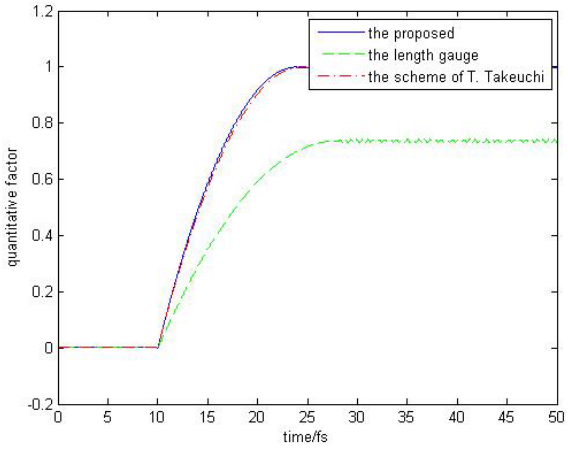

FIGURE 12. The quantitative factor Ω of the proposed scheme, the scheme of T. Takeuchi et al and the length gauge scheme.

The resultant variations of the factor Ω in the three schemes are shown in Figure 12. In the length gauge scheme, the factor increases rapidly when the pulses gradually raise. Then the factor stays at around 0.735 even after the pulse has disappeared. However, in our proposed and T. Takeuchi et al's scheme, the distributions indicate that the pulses of these two have high ability to modify the state into the wanted one. Some deviations of the proposed and Takeuchi's method are caused by the tiny differences of the spatiotemporal evolution of the wavefunction.

These results show that our proposed state controller is capable of switching the electron states stably and precisely, compared with the length gauge. And our system has a simpler numerical process than the system by T. Takeuchi et al when performing the same quality of the control performance.

V. CONCLUSION

In this paper, we have proposed a novel scheme of the quantum state control system, without any electromagnetic fields involved. The critical issue to this scheme is to design a new numerical model where the vector potential, the scalar potential and the wavefunction are tightly coupled. And the hybrid PML formulas are developed for the potential part. The performance of the PML is examined by the dipole test. Then the control ability of our proposed scheme and the other two scheme is studied and discussed. The results indicate that our scheme can perform an ideal control while of a simpler numerical process.

REFERENCES

[1] D. F. Walls, G. J. Milburn, and W. P. Schleich, "Quantum optics," *Phys. Today*, vol. 48, no. 6, pp. 55–56, 1995.
[2] R. Loudon, *The Quantum Theory of Light*. Oxford, U.K.: Clarendon, 1973.
[3] C. J. Bardeen *et al.*, "Quantum control of NaI photodissociation reaction product states by ultrafast tailored light pulses," *J. Phys. Chem. A*, vol. 101, no. 20, pp. 3815–3822, 1997.
[4] D. Brinks *et al.*, "Visualizing and controlling vibrational wave packets of single molecules," *Nature*, vol. 465, p. 905, Jun. 2010.
[5] C. Daniel *et al.*, "Deciphering the reaction dynamics underlying optimal control laser fields," *Science*, vol. 299, pp. 536–539, Jan. 2003.

[6] E. Lorin, S. Chelkowski, and A. Bandrauk, "A numerical Maxwell–Schrödinger model for intense laser–matter interaction and propagation," *Comput. Phys. Commun.*, vol. 177, pp. 908–932, Dec. 2007.
[7] A. Soriano, E. A. Navarro, J. A. Portí, and V. Such, "Analysis of the finite difference time domain technique to solve the Schrödinger equation for quantum devices," *J. Appl. Phys.*, vol. 95, no. 12, pp. 8011–8018, 2004.
[8] Y. Ohtsuki, H. Kono, and Y. Fujimura, "Quantum control of nuclear wave packets by locally designed optimal pulses," *J. Chem. Phys.*, vol. 109, pp. 9318–9331, 1998.
[9] S. Shi and H. Rabitz, "Quantum mechanical optimal control of physical observables in microsystems," *J. Chem. Phys.*, vol. 92, no. 1, pp. 364–376, 1990.
[10] W. Zhu, X. Zhao, and Y. Tang, "Numerical methods with a high order of accuracy applied in the quantum system," *J. Chem. Phys.*, vol. 104, no. 6, pp. 2275–2286, 1996.
[11] C. Gerry, P. Knight, and P. L. Knight, *Introductory Quantum Optics*. Cambridge, U.K.: Cambridge Univ. Press, 2005.
[12] Y. S. Joe, A. M. Satanin, and C. S. Kim, "Classical analogy of Fano resonances," *Phys. Scripta*, vol. 74, no. 2, pp. 259–266, 2006.
[13] I. Ahmed, E. H. Khoo, E. Li, and R. Mittra, "A hybrid approach for solving coupled maxwell and schrÃűdinger equations arising in the simulation of nano-devices," *IEEE Antennas Wireless Propag. Lett.*, vol. 9, pp. 914–917, 2010.
[14] K. Lopata and D. Neuhauser, "Multiscale Maxwell–Schrödinger modeling: A split field finite-difference time-domain approach to molecular nanopolaritonics," *J. Chem. Phys.*, vol. 130, no. 10, 2009, Art. no. 104707.
[15] Y. P. Chen, W. E. I. Sha, L. Jiang, M. Meng, Y. M. Wu, and W. C. Chew, "A unified Hamiltonian solution to Maxwell–Schrödinger equations for modeling electromagnetic field–particle interaction," *Comput. Phys. Commun.*, vol. 215, pp. 63–70, Jun. 2017.
[16] C. Cohen-Tannoudji, J. Dupont-Roc, and G. Grynberg, *Atom-Photon Interactions: Basic Processes and Applications: Claude Cohen-Tannoudji, Jacques Dupont-Roc, Gilbert Grynberg*. Hoboken, NJ, USA: Wiley, 1998, p. 678.
[17] T. Takeuchi, S. Ohnuki, and T. Sako, "Hybrid simulation of Maxwell–Schrödinger equations for multi-physics problems characterized by anharmonic electrostatic potential," *Prog. Electromagn. Res.*, vol. 148, pp. 73–82, Jul. 2014.
[18] T. Takeuchi, S. Ohnuki, and T. Sako, "Maxwell–Schrödinger hybrid simulation for optically controlling quantum states: A scheme for designing control pulses," *Phys. Rev. A, Gen. Phys.*, vol. 91, Mar. 2015, Art. no. 033401.
[19] C. J. Ryu, A. Y. Liu, W. E. I. Sha, and W. C. Chew, "Finite-difference time-domain simulation of the Maxwell–Schrödinger system," *IEEE J. Multiscale Multiphys. Comput. Techn.*, vol. 1, no. 2016, pp. 40–47, 2016.
[20] T. Takeuchi, S. Ohnuki, and T. Sako, "A quantum switching system manipulated by a light pulse pair designed in a Maxwell–Schrödinger hybrid algorithm," *URSI Radio Sci. Bull.*, vol. 356, pp. 13–19, Mar. 2016.
[21] C. Xiang, F. Kong, K. Li, and M. Liu, "A high-order symplectic FDTD scheme for the Maxwell-Schrödinger system," *IEEE J. Quantum Electron.*, vol. 54, no. 1, Feb. 2018, Art. no. 6100108.

CHEN XIANG was born in Yichang, China. He received the B.S. degree in electronic information science and technology from the Electronic Information School, Wuhan University, Wuhan, in 2014. He is currently pursuing the Ph.D. degree in electronic science and technology with the School of Information Science and Engineering, Shandong University, Jinan. His current research interests include computational electromagnetics and simulation of quantum phenomena.

FANMING KONG received the B.S. and M.S. degrees in electrical engineering from Shandong University, Jinan, China, in 1991 and 1994, respectively, and the Ph.D. degree from the School of Physics, Shandong University, in 1999, where he joined the Department of Electrical Engineering, in 1999, and currently a Professor with the School of Information Science and Engineering. His current research interests include computational electromagnetics and numerical methods for plasmonic, and photonic devices modeling and design.

KANG LI (M'09) was born in Jinan, China, in 1962. He received the B.S. and M.S. degrees in electrical engineering and the Ph.D. degree in optical engineering from Shandong University, Jinan, in 1984, 1987, and 2006, respectively, where he is currently a Professor with the School of Information Science and Engineering. His current research interests include computational electromagnetics and fiber-optic communications.

MENG LIU was born in Shandong, China. He received the B.S. degree in electronic information engineering and the M.S. degree in physical electronics from Qufu Normal University, in 2004 and 2007, respectively, and the Ph.D. degree from the School of Information Science and Engineering, Shandong University, in 2017. He joined the School of Physics and Electrical Engineering, Qilu Normal University, in 2017, where he is currently a Lecturer. His research interests include the theory and method of computational electromagnetics, and the simulation of semiconductor devices. He is currently involved in research on modeling and design of high-power, and high-efficiency LEDs.